Aspects of the upstream region in a plasma jet with dielectric barrier discharge configurations*

Li Xue-Chen(李雪辰)†, Jia Peng-Ying(贾鹏英),
Yuan Ning(袁 宁), and Chang Yuan-Yuan(常媛媛)

College of Physics Science & Technology, Hebei University, Baoding 071002, *China*

(Received 26 July 2011; revised manuscript received 25 August 2011)

A plasma column with a length of about 65 cm is generated in the upstream region of a plasma jet using dielectric barrier discharge configurations. The effects of experimental parameters such as the amplitude of the applied voltage and the driving frequency are investigated in aspects of the plasma column by the optical method. Results show that both the plasma length and the propagating velocity, as well as the discharge current, increase with the increase in the applied voltage or its frequency. The discharge mechanism is analysed qualitatively based on streamer theory, where photo-ionization is important. Furthermore, optical emission spectroscopy is used to investigate the electric field intensity of the upstream region.

Keywords: dielectric barrier discharge, plasma jet, upstream region, optical emission spectroscopy

PACS: 52.80.Tn, 52.80.Hc, 52.80.Mg **DOI:** 10.1088/1674-1056/21/4/045204

1. Introduction

Atmospheric pressure plasmas have been the focus of low-temperature plasma research, and there is a trend that atmospheric pressure plasma sources will replace the plasma sources operated in vacuum systems in industrial plasma engineering.[1] One kind of atmospheric pressure plasma source, a cold plasma jet generated in atmospheric pressure discharge, represents a rapidly developing technology.[2] Cold plasma sources usually work in remote mode, which means that they can generate a plasma plume in the plasma application region. Moreover, cold plasma jets demonstrate many desirable properties, including low gas temperature, easy plasma dynamics control and high reactive chemical species.[2,3] Aspects of plasma plume (plasma column) have been investigated using various structures (e.g., single electrodes, two electrodes with a floating electrode, ring-to-plate electrodes, etc.).[4] The plasma jets can be generated in many different gases, accompanied with different electrical excitations. These plasma jets include dc jets employing air and nitrogen,[5] kilohertz frequency pulsed and sinusoidal jets,[6−8] and radio frequency or microwave excited jets.[9] Depending on the jet configurations and electrical excitation, the aspects of plasma plumes may differ from each other significantly. A plasma plume is often several centimeters long in an argon jet with dielectric barrier discharge (DBD) configurations.[10] A plasma plume up to 11 cm long was generated in helium in a DBD with needle-to-ring electrodes by a kilohertz excitation.[11] A plasma column with a length of about 55 cm was produced in argon with twin injection-needle electrodes,[12] and an over 165 cm long argon plasma plume was generated with a single electrode.[4] The plasma plumes mentioned above are all generated in the downstream region of the gas flow. Plasma plumes have been observed in the upstream region,[10] however, the plasma plume aspects in the upstream region and the physical mechanisms of generated plasma propagation have not been understood. These aspects are therefore investigated in this paper.

2. Experimental setup

The experimental device is shown in Fig. 1. The plasma jet originates from the DBD, which is composed of two coaxial electrodes: a tungsten cylindri-

*Project supported by the National Natural Science Foundation of China (Grant Nos. 10805013 and 51077035), the Natural Science Foundation of Hebei Province, China (Grant Nos. A2009000149 and A2011201132), the Key Project of Chinese Ministry of Education, China (Grant No. 210014), the Science Funds of Hebei Education Department for Outstanding Youth (Grant No. Y2011120), and the Hebei University Funds for Distinguished Young Scientists.

†Corresponding author. E-mail: xcli@mail.hbu.edu.cn

© 2012 Chinese Physical Society and IOP Publishing Ltd

cal electrode that is surrounded by the other electrode (water electrode). The diameter of the tungsten electrode is 1 mm. The tungsten electrode is coaxially surrounded by two glass tubes, each with a wall thickness of 1 mm. Water filled between the two tubes is used as the water electrode. The active length of the barrier discharge electrode is about 12.8 cm.

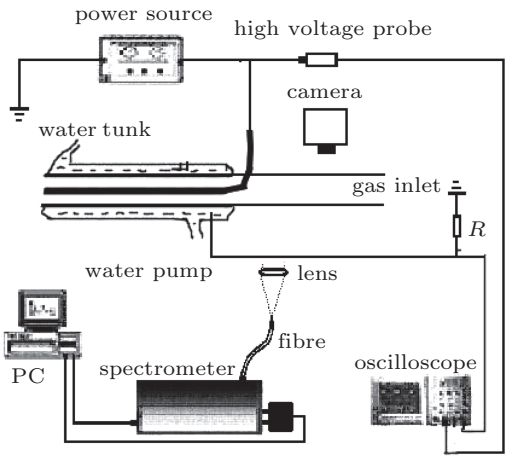


Fig. 1. Schematic diagram of the experimental setup.

Argon (99.99%) flows along the gap between the tungsten electrode and the inner glass tube, and the gas gap width is about 3 mm. The inner glass tube is about 70 cm long in the upstream region of the DBD electrode. The gas flow rate can be adjusted from 0 L·min^{-1} to 10 L·min^{-1}. During the experiments, the tungsten electrode is connected to the high voltage output of the power supply, and the water electrode is grounded through a small resistance (50 Ω) to measure the discharge current. A sinusoidal ac power supply with a maximum peak voltage of 10 kV and a frequency of 30–60 kHz is used. The applied voltage can be detected by a high voltage probe (Tektronix P6015A). Both the applied voltage and the discharge current are recorded with an oscilloscope (Tektronix DPO4054). A digital camera (Konica Z2) is used to record the discharge images, and the exposure time is 8 ms in our experiments. For spatially resolved measurements, an imaging system is used. One end of an optical collimator is tightly pressed into the discharge tube to collect the discharge light emission from an area with a diameter of about 3 mm. A photomultiplier tube (RCA7265) is placed at the other end of the optical collimator to detect the light emissions. Optical emission spectroscopy is used to measure the emission spectra from the discharge, and a spectrometer equipped with a CCD detector (ACTON SP2758) is used to acquire the spectrum with a grating of 2400 grooves mm^{-1}.

3. Results and discussion

Raising the voltage of the power supply to more than 600 V, DBD can be ignited in the intra-electrode region. A plasma plume can be observed in the downstream region. As the voltage is increased to a certain value (about 3.5 kV), discharges start to appear in both the downstream and the upstream regions. Figure 2 shows an image of the DBD and its upstream region. Obviously, a longer plasma column can be generated in the upstream region than in the downstream region because the diffusion of ambient air will quench the downstream discharge.

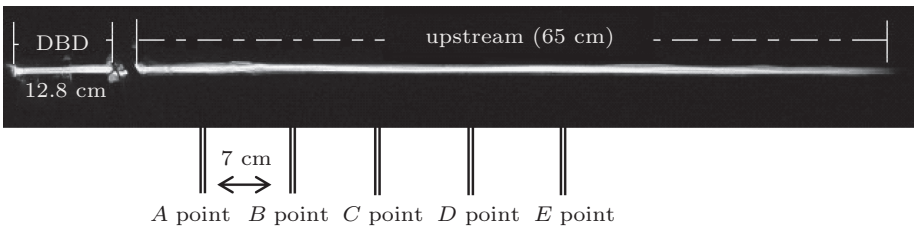


Fig. 2. An image of the DBD and the upstream discharge with an exposure time of 8 ms. Other parameters are $U_{\rm p} = 8.5$ kV and $f = 50$ kHz.

Figure 3 shows the waveforms of the applied voltage and the discharge current. It can be found that the discharge current shows a pulse per half cycle of the applied voltage: the pulses for positive half cycle and negative half cycle of the applied voltage are asymmetric with respect to each other. This phenomenon may result from the asymmetric configurations of the two discharge electrodes. Furthermore, figure 3 indicates that the amplitude and the width of the discharge pulse increase with increasing applied voltage. The amplitude of the discharge current also increases with increasing driving frequency, as shown in Fig. 4.

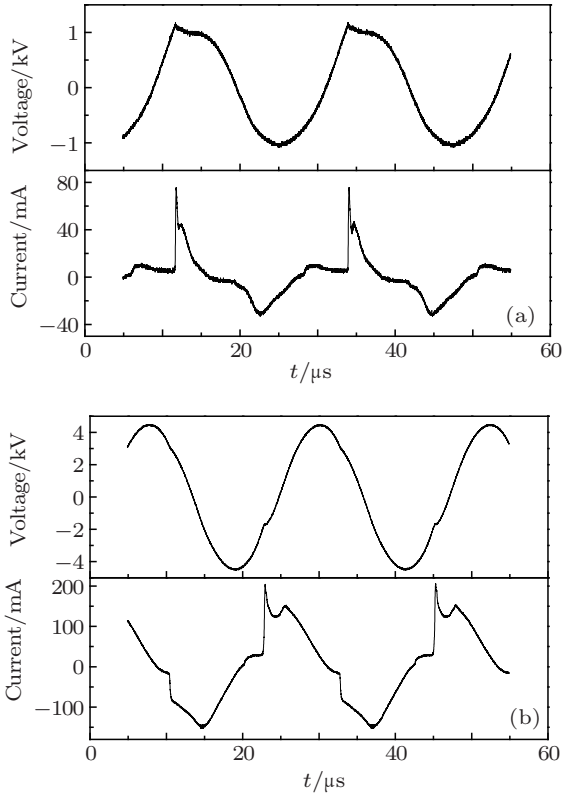


Fig. 3. Waveforms of the applied voltage and the discharge current at (a) $U_{\rm p} = 1.0$ kV and (b) $U_{\rm p} = 4.5$ kV.

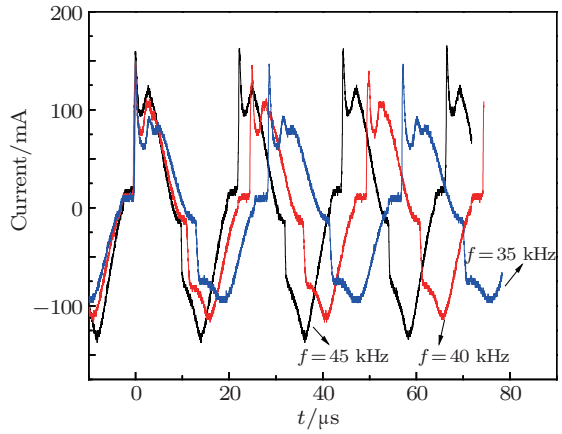


Fig. 4. (colour online) Waveforms of the discharge current under different frequencies of the applied voltage ($U_{\rm p} = 3.5$ kV).

It is easy to understand the phenomena demonstrated in Figs. 3 and 4. It is well known that the wall charges in DBD have double effects on the discharge. They can quench the discharge in this half cycle and this helps the next breakdown in the forthcoming half cycle. Therefore, more wall charges must be accumulated on the dielectric to quench the discharge when $U_{\rm p}$ is increased. Consequently, the discharge current increases if $U_{\rm p}$ is increased at a constant driving frequency. For the same reason, the number of wall charges remains almost constant when the driving frequency is increased at a constant $U_{\rm p}$. The time for accumulating the number of wall charges decreases with increasing driving frequency. Therefore, the discharge current increases with increasing driving frequency.

It has been found in our experiment that the length of the plasma column in the upstream region increases with the increase in $U_{\rm p}$ or the driving frequency, which is shown in Fig. 5. It is worthwhile pointing out that the curve consists of two lines, and their slope rates are different. The length of the plasma column in the upstream region has little relevance on the gas flow rate, while the gas flow rate can greatly influence the length of the plasma plume in the downstream region.[10] The generation of a plasma column in the upstream region is an electric discharge phenomenon rather than a gas flow phenomenon. To understand the mechanism of upstream region discharge, a spatially resolved measurement of light emission is conducted in our experiment. Figure 6(a) shows the waveforms of the applied voltage, the total light emission signal and the light signals emitted from five different discharge areas, each with a diameter of about 3 mm. From A to E, the distances away from the DBD increase, as shown in Fig. 2.

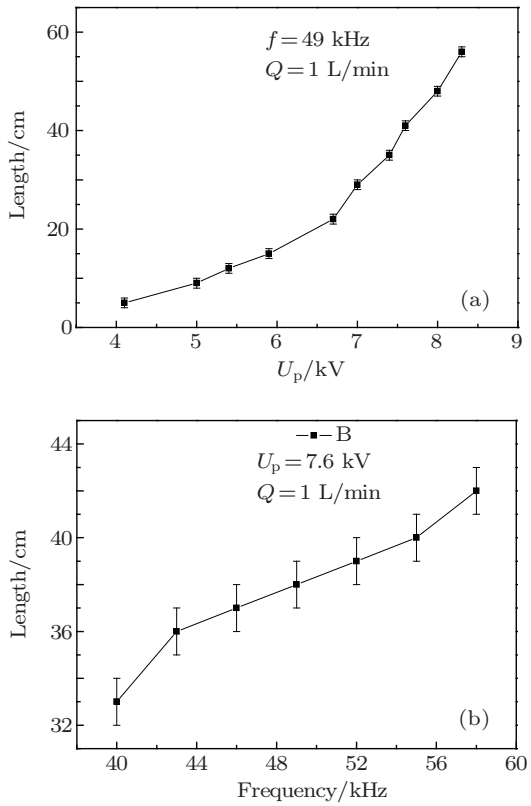


Fig. 5. The length of the upstream plasma as a function of $U_{\rm p}$ and driving frequency, separately.

In each half cycle, the total light emission signal shows a hump with a width of about a half cycle of the applied voltage. The light emission signal from each area shows a pulse with a width of about 3 μs. It is interesting that the time lag in each half cycle increases with the increase in distance away from the DBD. It can be deduced from Fig. 6(a) that the discharge propagation in the upstream region is similar to that in the downstream region, where a plasma bullet is introduced to describe the discharge. For the downstream region, bullet-like behaviours are found in the positive discharge and sometimes can be found in the negative discharge.[13] However, bullet-like behaviours are found at both positive and negative half cycles for the upstream region. The 3μs width of the light emission signal in each area results from the afterglow discharge after the wave front of the streamer has passed away, which is similar to the behaviour of the downstream discharge reported by Shashurin *et al.*[14] Because area A is near the DBD, the light pulse of A always appears at the rising edge of the applied voltage. This phenomenon implies that the plasma bullet always leaves the DBD at the rising edge of the applied voltage. The time lag versus the distance from the DBD is used to calculate the propagation velocity of the discharge, which is shown in Fig. 6(b). It can be found in Fig. 6(b) that the time lag increases linearly with the increase in distance, and the slope rate can give the discharge development velocity.

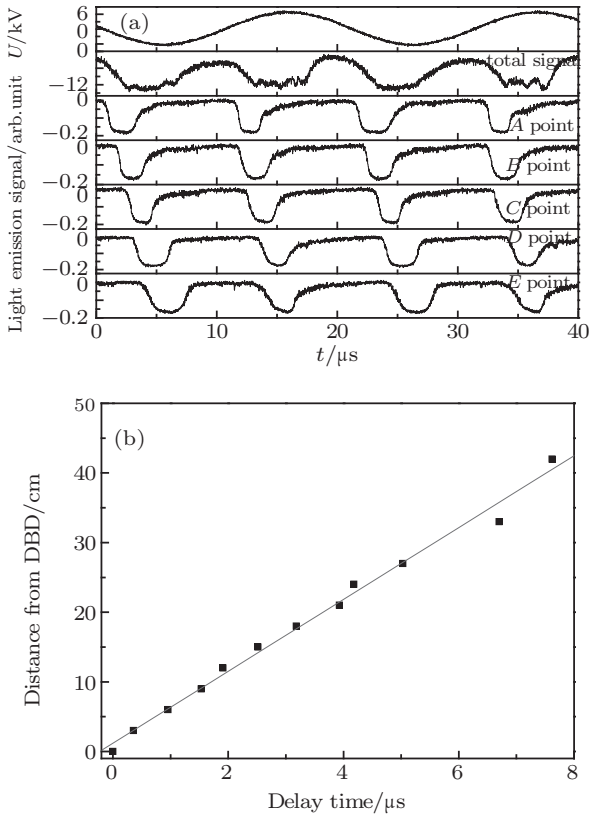


Fig. 6. (a) Waveforms of the applied voltage, the total light emission signal and the light signals emitted from five different areas, each with a diameter of about 3 mm. From A to E, the distances away from the DBD increase. (b) The relations between the upstream position and the delay time, with the other parameters being $U_{\rm p} = 6.3$ kV and $f = 50$ kHz.

By this method, the discharge propagation velocity as a function of $U_{\rm p}$ and driving frequency is investigated in the upstream region. As shown in Fig. 7, the propagation velocity increases with the increase in the applied voltage or driving frequency in the upstream region. The length of the plasma bullet can be estimated by multiplying the propagating velocity with the pulse width shown in Fig. 6(a). The length of the plasma bullet in our experiment is about 20 cm.

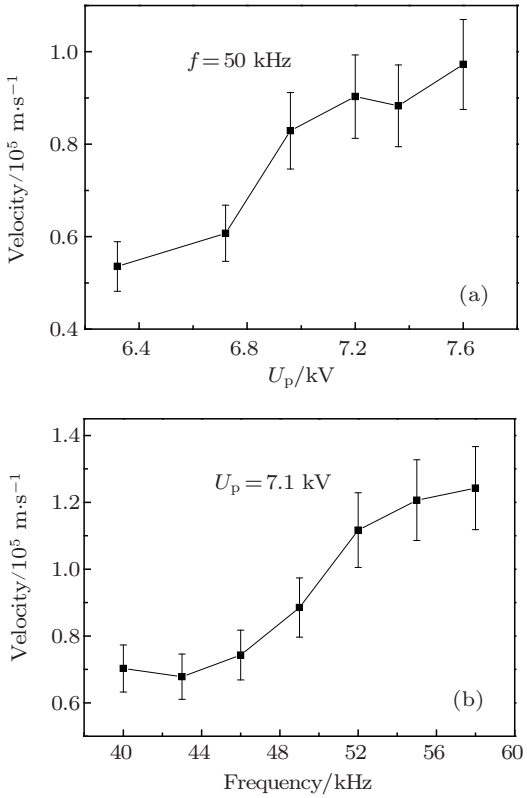


Fig. 7. Discharge propagation velocity as a function of $U_{\rm p}$ and driving frequency.

As is well known, the formation of a plasma bullet is involved with the streamer discharge mechanism and the photo-ionization theory proposed by Dawson. Because the anode-directed streamer is not well understood, the cathode-directed streamer at the positive half cycle will be discussed. According to Meek's criterion, the streamer will be formed when the electric field formed by spatial charges is comparable to the applied electric field. For the cathode-directed

streamer, it is postulated that the streamer tip consists of numerous positive ions. Photons emitted from the streamer tip create photoelectrons at a small distance in front of the tip. The photoelectrons will be accelerated toward the positive ions and a small electron avalanche is formed under the resulting electric field, composed of the applied electric field and the spatial electric field formed by positive ions. If the resulting electric field is high enough, the process mentioned above will continue including new photoionization and new electron avalanche. The afterglow discharge will be sustained at this position until the resulting electric field is lower than a certain value because of the accumulation of a new layer of spatial charges. Obviously, afterglow discharge will be observed after the streamer has broken down, which is shown in Fig. 6(a), and consequently the new layer of positive ions will create new breakdown at a small distance ahead of the layer of ions. This layer of ions is the wave front of streamer propagation. Therefore, the positively charged ions have two effects on the discharge.

These positively charged ions can help the discharge ahead of it and quench the discharge behind it. As mentioned above, the plasma bullet leaves the DBD at the rising edge of the applied voltage. The increase rate in the applied electric field increases with the increase in $U_{\rm p}$ or driving frequency for the streamer inception. With the increase rate increasing, more spatial charges must be left to quench the afterglow discharge, leading to an increased resulting electric field ahead of the layer. The drifting velocity of electrons increases with the increasing electric field intensity. The increase in drifting velocity contributes to the increase in discharge propagation velocity. Therefore, the propagation velocity increases with the increase of $U_{\rm p}$ or driving frequency in the upstream region. Furthermore, with the number of original spatial ions increasing, the resulting electric field will increase for the initial streamer formation. With the number of spatial ions increasing and the electric field augmenting, the streamer tends to propagate a farther distance.

To validate the theory mentioned above, the electric field is obtained as a function of experimental parameters. The variation in the intensity ratio of spectral lines is often used to represent the change in electron energy.[15,16] The spectral lines 772.4 nm ($2P_2 \rightarrow 1S_3$) and 763.5 nm ($2P_6 \rightarrow 1S_5$) from Ar I are chosen to investigate the electron energy, which is shown in Fig. 8(a). In the plasma region, Ar ($2P_2$ state) is populated mainly by the direct collisions between ground state Ar and electrons higher than 13.35 eV. The $2P_6$ state of Ar is populated mainly by the direct collisions with electrons higher than 13.19 eV. Therefore, if the intensity ratio of 772.4 nm to 763.5 nm is changed, this means a change in average electron energy. The electron energy is determined by the resulting electric field. Consequently, the intensity ratio of 772.4 nm to 763.5 nm can be used to present the electric field. As shown in Figs. 8(b) and 8(c), the intensity ratio increases with the increase of $U_{\rm p}$ or driving frequency. These results are consistent with the phenomena shown in Figs. 5 and 7.

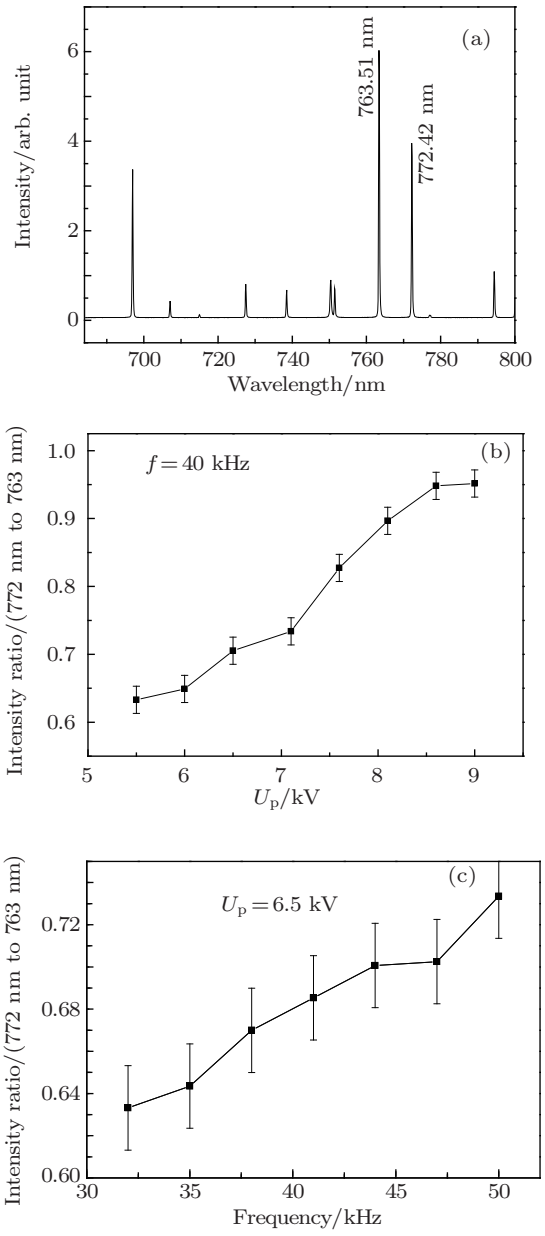


Fig. 8. (a) Optical emission spectrum in a range from 680 nm to 800 nm, and the intensity ratio (772.42 nm to 763.51 nm) as a function of $U_{\rm p}$ (b) and driving frequency (c), separately.

4. Conclusion

A plasma column with a length of about 65 cm is generated in the upstream region of a plasma jet using dielectric barrier discharge configuration. An optical method is used to investigate the aspects of the plasma column in the upstream region. The results show that both the plasma length and the developing velocity, as well as the discharge current, increase with the increase of $U_{\rm p}$ or its frequency. The discharge mechanism is analysed qualitatively based on photo-ionization and streamer propagation. It is found that the formation of the plasma column in the upstream region results from the streamer mechanism where photo-ionization is important. The plasma length and the propagating velocity can be explained qualitatively each as a function of experimental parameters. Furthermore, optical emission spectroscopy is used to validate the qualitative explanation.

References

[1] Jeong J Y, Babayan S E, Tu V J, Park J, Henins I, Hicks R F and Selwyn G S 1998 *Plasma Sources Sci. Technol.* **7** 282

[2] Li X C, Yuan N, Jia P Y and Chen J Y 2010 *Phys. Plasmas* **17** 093504

[3] Yuri R P 1991 *Gas Discharge Physics* (New York: Springer)

[4] Chen L W, Zhao P, Shu X S, Shen J and Meng Y D 2010 *Phys. Plasmas* **17** 083502

[5] Feng H, Sun P, Chai Y, Tong G, Zhang G J, Zhu W and Fang J 2009 *IEEE Trans. Plasma Sci.* **37** 121

[6] Li X C, Yuan N, Jia P Y, Chang Y Y and Ji Y F 2011 *Acta Phys. Sin.* **60** 125204 (in Chinese)

[7] Li X C, Dong L F, Zhao N and Yin Z Q 2007 *Appl. Phys. Lett.* **91** 161507

[8] Chen G L, Chen S H, Chen W X and Yang S Z 2008 *Chin. Phys.* B **17** 4568

[9] Kim J and Terashima K 2005 *Appl. Phys. Lett.* **86** 191504

[10] Li Q, Li J T, Zhu W C, Zhu X M and Pu Y K 2009 *Appl. Phys. Lett.* **95** 141502

[11] Lu X P, Jiang Z H, Xiong Q, Tang Z Y, Hu X W and Pan Y 2008 *Appl. Phys. Lett.* **92** 081502

[12] Hong Y C, Cho S C and Uhm H S 2007 *Appl. Phys. Lett.* **90** 141501

[13] Walsh J L, Iza F, Janson N B, Law V J and Kong M G 2010 *J. Phys.* D: *Appl. Phys.* **43** 075201

[14] Shashurin A, Shneider M N, Dogariu A, Miles R B and Keidar M 2009 *Appl. Phys. Lett.* **94** 231504

[15] Choi J H, Lee T I, Han I, Baik H K, Song K M, Lim Y S and Lee E S 2006 *Plasma Sources Sci. Technol.* **15** 416

[16] Li X C, Jia P Y, Yuan N, Fang T Z and Wang L 2011 *Phys. Plasmas* **18** 043505